

Supporting Information

Zn₃V₂O₈ hexagon nanosheets: a high-performance anode material for lithium-ion batteries

Contents

Experimental Section: The synthesis of Zn₃V₂O₈ nanoparticles.

Figure S1. TG analysis of Zn₃V₂O₇(OH)₂·2H₂O.

Figure S2. XPS images of Zn2p_{3/2}, (A) as-prepared; (B) discharge down to 0.01V

Figure S3. XPS images of V2p_{3/2}, (A) as-prepared; (B) discharge down to 0.01V

Figure S4. (A) the crystal structure of Zn₃V₂O₈, perspective views from (B)a, (C)b, (D)c planes, respectively, (E)a planes of 4×4×4 supercell.

Figure S5. XRD patterns of Zn₃V₂O₈ nanoparticles.

Figure S6. The SEM image of Zn₃V₂O₈ nanoparticles.

Figure S7. Nitrogen adsorption and desorption isotherms of Zn₃V₂O₈ hexagon nanosheets, with the corresponding pore-size distribution (inset) calculated by the BJH method from the desorption branch.

Figure S8. Nitrogen adsorption and desorption isotherms of Zn₃V₂O₈ nanoparticles, with the corresponding pore-size distribution (inset) calculated by the BJH method from the desorption branch.

Figure S9. The SEM image of Zn₃V₂O₈ nanosheets electrode after 150 charge/discharge cycles.

Experimental Section:

Synthesis of $\text{Zn}_3\text{V}_2\text{O}_8$ nanoparticle

All chemicals used were analytic grade reagents used without further purification. In a typical process, 0.75mmol ZnAc_2 and 0.5mmol NH_4VO_3 were grinding evenly at room temperature in air. At last the powder was calcined at 600°C in air for 12 h to yield the final products.

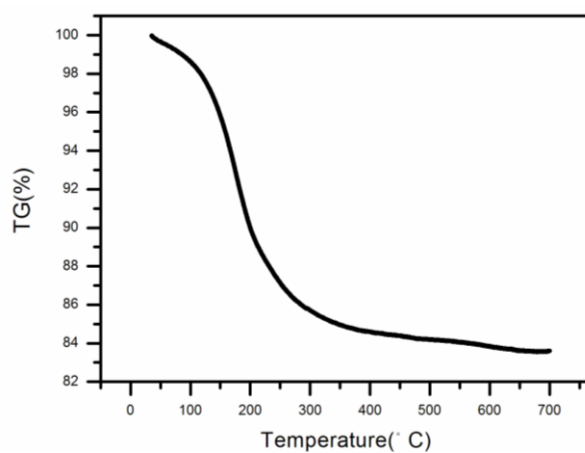


Figure S1. TG analysis of $\text{Zn}_3\text{V}_2\text{O}_7(\text{OH})_2\cdot 2\text{H}_2\text{O}$.

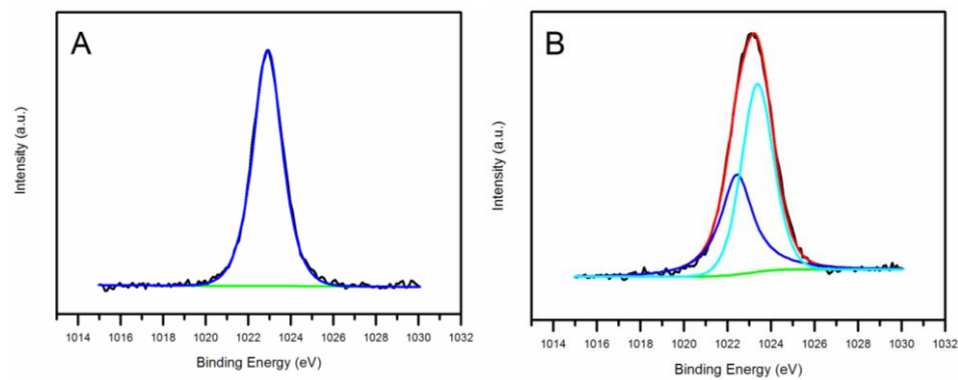


Figure S2. XPS images of $\text{Zn}2p_{3/2}$, (A) as-prepared; (B) discharge down to 0.01V

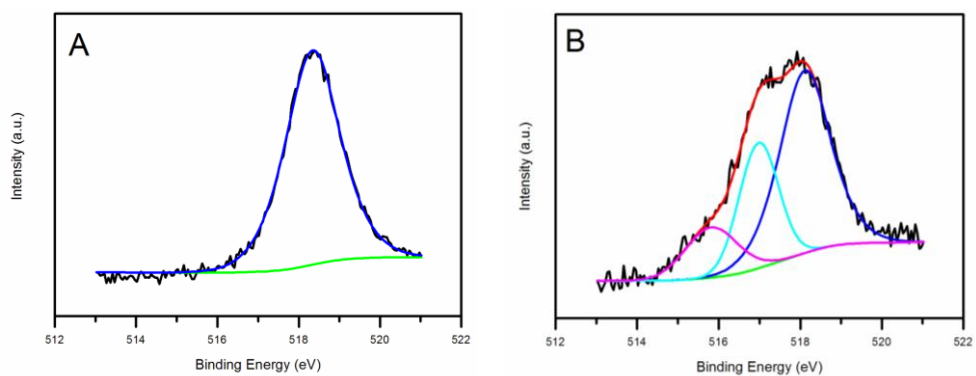


Figure S3. XPS images of $V2p_{3/2}$, (A) as-prepared; (B) discharge down to 0.01 V

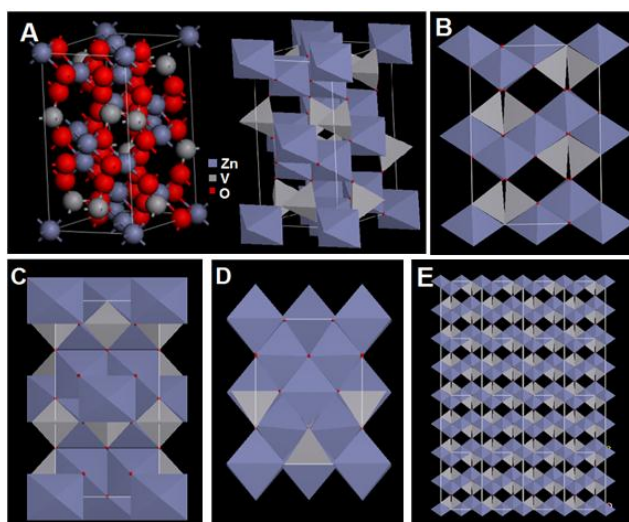


Figure S4. (A) the crystal structure of $Zn_3V_2O_8$, perspective views from (B)a, (C)b, (D)c planes, respectively, (E)a planes of $4 \times 4 \times 4$ supercell.

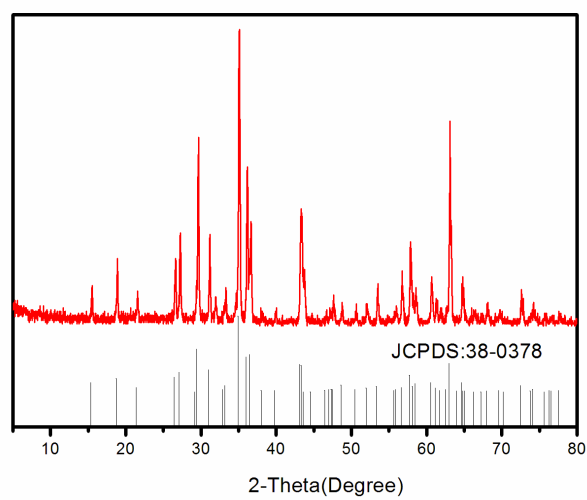


Figure S5. XRD patterns of Zn₃V₂O₈ nanoparticles.

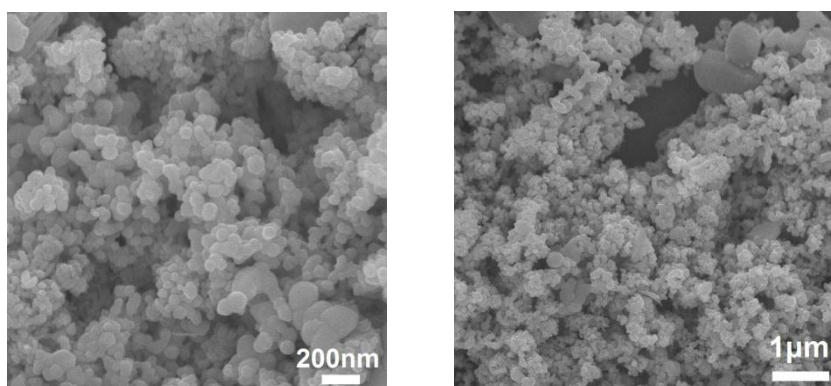


Figure S6. The SEM image of Zn₃V₂O₈ nanoparticles.

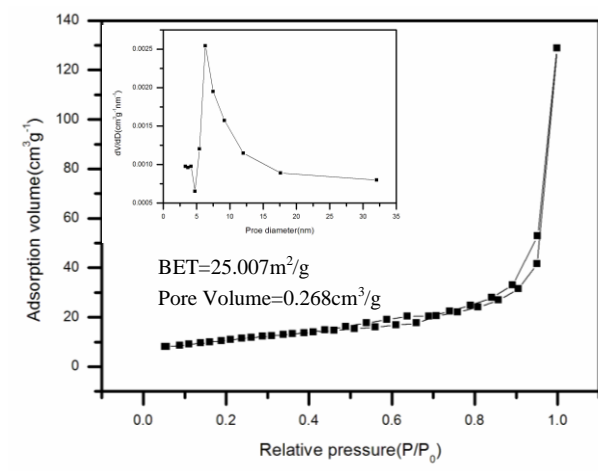


Figure S7. Nitrogen adsorption and desorption isotherms of $\text{Zn}_3\text{V}_2\text{O}_8$ hexagon nanosheets, with the corresponding pore-size distribution (inset) calculated by the BJH method from the desorption branch.

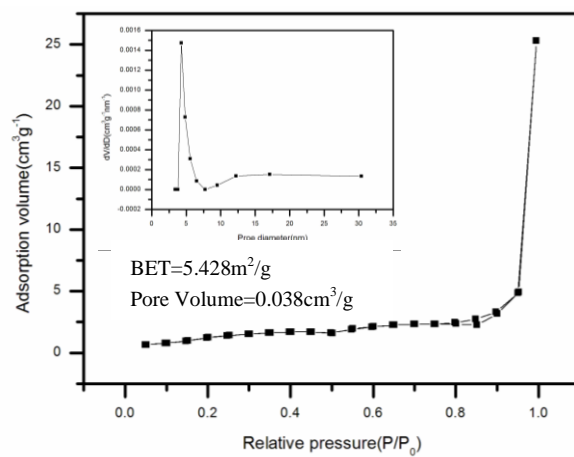


Figure S8. Nitrogen adsorption and desorption isotherms of $\text{Zn}_3\text{V}_2\text{O}_8$ nanoparticles, with the corresponding pore-size distribution (inset) calculated by the BJH method from the desorption branch.

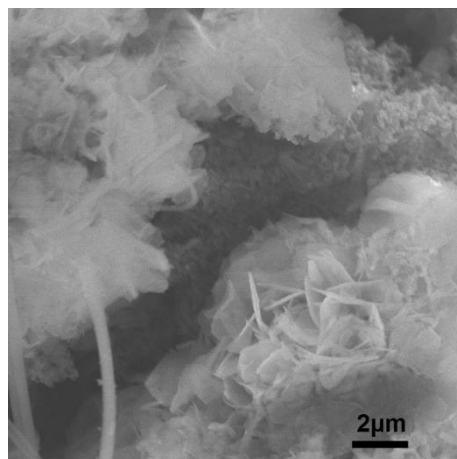


Figure S9. The SEM image of Zn₃V₂O₈ nanosheets electrode after 150 charge/discharge cycles.